

**“Design Fabrication and Testing of a Novel Multifunctional
Wound Healing Device”**



Submitted by: Mariam Mir

NUST201362084MSMME62413F

Supervisor: Dr Umar Ansari

Department of Biomedical Engineering and Sciences

NUST School of Mechanical and Manufacturing Engineering (SMME)

National University of Sciences and Technology

Islamabad, Pakistan

June, 2015

Declaration

It is hereby declared that this research study has been done for partial fulfillment of requirements for the degree of Master of Sciences in Biomedical Engineering. This work has not been taken from any publication. I hereby also declare that no portion of the work referred to in this thesis has been submitted in support of an application for another degree or qualification in this university or other institute of learning.

Mariam Mir



CERTIFICATE OF APPROVAL

TH-4

We hereby recommend that the dissertation prepared under our supervision by:

Name of Student: Mariam Mir Registration No: NUST201362084MSMME62413F

Title: Design Fabrication and Testing of a Novel Multifunctional Wound Healing Device

be accepted by the School of Mechanical and Manufacturing Engineering, Department of Biomedical Engineering and Sciences, National University of Sciences and Technology (NUST), Islamabad in partial fulfillment of the requirements for the award of MS degree with Grade A.

Examination Committee Members

Dr Murtaza Najabat Ali

BMES, SMME

Dr Nabeel Anwar

BMES, SMME

Dr Nosheen Fatima

BMES, SMME

Supervisor's Name: Dr. Umar Ansari

BMES, SMME

Head of Department

BMES, SMME

Date

COUNTERSIGNED

Date: _____

Dean/Principal

Dedicated to:

My parents; without their encouragement and support, I would not have been able to successfully complete this research.

My supervisor, Dr. Umar Ansari; I will be forever grateful to him for all his valuable time and patience; and for all that he has taught me.

Acknowledgements

All praises to Almighty Allah.

My parents, for their kindness and support.

My supervisor Dr Umar Ansari, for his time and effort in contributing to and shaping my research; and his uncanny problem solving abilities. He has been a brilliant supervisor.

My co-supervisor, Dr Murtaza Najabat Ali, for his kind guidance and support, throughout my academic period in NUST. A lot of what I have achieved is because of him.

My fellow researchers and friends, especially Tehreem Jamil and Abida Batool. These people have been a huge support for me throughout my time in NUST, and I am very thankful to them for this.

PUBLISHED WORK:

- Murtaza Najabat Ali, Faisal Amin, Umar Ansari, Muhammand Asim Minhas, Mariam Mir, Wakeel Shahid (2014), “Anisotropic Coronary Stent Device: Fabrication and Structural Analysis”, Journal of Applied Biomaterials and Functional Materials (Published), Impact Factor 1.5
- Mariam Mir, Murtaza Ali, Umar Ansari and Javaria Sami (2014), “Review of Mechanics and Applications of Auxetic Structures”, Advances in Materials Science and Engineering (Published)
- Faisal Amin, Murtaza Najabat Ali, Mariam Mir, Umar Ansari (2014), “Emerging Approach for Treating Complications Associated with Pertrochanteric Fractures: A Review”, Minerva Orthopeda E Traumatologica (Published)
- Zainab Munib, Murtaza Najabat Ali, Umar Ansari, Mariam Mir (2014), “Auxetic Polymeric Bone Stent for Tubular Fractures, Design Fabrication and Structural Analysis”, International Journal of Polymeric Materials (Accepted)
- Seemab Mehmood, Murtaza Najabat Ali, Umar Ansari, Mariam Mir, Munezza Ata Khan (2015), “Auxetic Polymeric Bone Plate as Internal Fixator for Long Bone Fractures: DESIGN, FABRICATION AND STRUCTURAL ANALYSIS”, Technology and Health Care (Accepted)
- Mariam Mir, Umar Ansari, Murtaza Ali (2015), “A Macro-Scale Model of a Tunable Drug Dispensation Device for Enhanced Wound Healing”, Journal of Applied Biomaterials and Functional Materials” (Accepted)
- Mariam Mir, Murtaza Najabat Ali, Umar Ansari, Javeria Sami (2015), “Structure and Motility of the Esophagus from a Mechanical Perspective”, Esophagus, the official journal of the Japan Esophageal Society (Accepted)
- Mariam Mir, Umar Ansari, Murtaza Najabat Ali (2014), “An Appraisal of the Biomaterials Used in Wound Management Applications”, Journal of Applied Biomaterials and Functional Materials (Submitted)
- Javeria Sami, Murtaza Najabat Ali, Umar Ansari, Mariam Mir (2015), “Role of Stent Disappearance in Improving the Results of Stenting in Coronary Arteries: A Comparative Perspective”, Expert Review of Medical Devices (Submitted)
- Tehreem Jamil, Umar Ansari, Murtaza Najabat Ali, Mariam Mir (2015), “A Review on Biomechanical and Treatment Aspects Associated with Anterior Cruciate ligament”, IRBM - Innovation and Research in BioMedical Engineering (Submitted)
- Mariam Mir, Muhammad Hassan ul Iftikhar, Umar Ansari, Murtaza Najabat Ali (2015) “Electromechanically Actuated Multifunctional Wireless Auxetic Device for Wound Management”, Journal of Applied Biomaterials and Functional Materials (JABFM) (Submitted)

PATENTS

- Ansari, Umar; Ali, Murtaza; Mir, Mariam. Intelligent Bandage with Drug Dispensation and Adjustable Porosity for Topical Wounds. 291/2014, 31/3/2014 (Patent Filed)
- Ansari, Umar; Ali, Murtaza; Mir, Mariam. A Multifunctional Device that promotes Wound Healing through Drug Delivery and Exudate Removal. 711/2014, 10/10/2014 (Patent Filed)

Table of Contents

Abstract.....	10
Introduction.....	12
Phase I.....	13
Phase II.....	14
Literature Review.....	15
Physiology of wound healing.....	16
Occlusive/Polymeric dressings for wound healing.....	17
Synthetic Polymer films and wound dressings.....	18
Materials and Methods.....	20
Phase I.....	20
Phase II.....	24
Results and Discussion.....	32
Phase I.....	32
Phase II.....	40
Conclusion.....	49
References.....	50

List of Figures and Tables

Figure/Table	Title	Page No.
Figure 1	Macro Model of Mechanism	21
Figure 2a	Schematic showing direction of mechanism expansion	22
Figure 2b	Schematic showing interlocked pins and slit width	22
Figure 3 a,b	Laminate arrangement of device components	24
Figure 4	CAD model-features in surface A and B of the device	25
Figure 5	Auxetic behavior of rotating squares geometry	26
Figure 6a	Schematic-pulley mechanism	27
Figure 6b	Schematic- lead-screw mechanism	27
Figure 7	Flexible skin facing surface of device	29
Figure 8	Laminate arrangement of fabricated device	30
Figure 9	Image processing results	32
Figure 10	Graph-parabolic pattern of dimensions for extended unit cells	33
Figure 11	Elution of drug particles from open pores of the film	34
Figure 12	Testing of macro-model	34
Figure 13	Auxetic Film in expanded and un-expanded form	37
Figure 14	Schematic explaining Mathematical Model	38
Figure 15	Graphical representation of results – pulley mechanism	42
Figure 16	Graphical representation of results – lead screw mechanism	43
Figure 17	Graphical representation of Quantity of Simulated Wound Exudate drawn up	45
Table 1	List of Notations in Mathematical Model 1 and 2	36
Table 2 and 3	Qty of drug administered-pulley mechanism	40
Table 4	Comparison of rate of release for both data sets	44
Table 5	Qty of simulated wound exudate	44

Abstract:

Auxetic materials tend to exhibit stretching in the direction of the applied load as well as in the perpendicular direction. This may be an inherent property of the material, or it might be a particular structural characteristic, that confers it with auxetic properties. The auxetic properties of a rotating squares auxetic design has been utilized in tandem with a stretching mechanism to manufacture a device that offers the advantages of adjustable pore size and hence tunable drug delivery characteristics. The auxetic polyurethane film has been fabricated through the polymer casting technique. The ABS plastic mould for polymer casting was made through additive manufacturing. Stereolithography has been used for fabrication of the mechanism that controls pore size of the polymeric auxetic film. A laminate arrangement of the film and the mechanism has been devised, through which the movement of the mechanism controls the stretching of the auxetic film underneath. Results have been analyzed through image processing. It has been observed that a two-dimensional increase (in length and width) of the auxetic film takes place that corresponds to an increase in pore size of the film. Several mathematical correlations have been drawn up, and it may be concluded that the first factor controlling drug release kinetics would be the pore size of the film. In Phase I, we have explored the aspect of such a prototype, which has the potential of being used as a device for controlled drug delivery as well as a smart bandage that may enhance wound healing in a chronic wound treatment.

Phase II of the research study continues along the same lines, but addresses and attempts to resolve the limitations inherent in the work previously done. In this study we have described the design and fabrication of a more life scale version of the wound healing device; this device caters to both the aspects of controlled drug delivery and exudate removal for chronic wounds. The device has been fabricated using a biocompatible polymer cast with structural features machined and modified through Laser Cutting. Subsequent tests have been conducted to account for the functionality of the device in controlled drug delivery. In this respect, two electronically actuated mechanisms (the lead-screw and pulley mechanisms) have been explored; these are miniaturized versions that fit compactly in the device structure and can be effectively controlled with a microcontroller set up. An auxetic polymeric film has been employed to limit the amount of drug being administered to the wound site. Drug delivery results for both

mechanisms have been compared and assessed. The exudate removal efficiency of the device has been assessed through several simple tests using simulated wound exudate.

Introduction:

An ideal wound healing dressing should minimize infection and pain, promote re-epithelialization and assist in the maintenance of a relatively moist environment for rapid wound healing. Needless to say, there are several wound dressings in the market that ‘approach’ definition of ideal, but no currently available dressing fulfills all of the criteria mentioned above [24]. In order for rapid wound healing to take place, it is mandatory that bacterial colonization of the wound is prevented to a large degree as infection delays wound healing and large vessel angiogenesis, due to prolonged inflammation times[25][26]. Medicated wound dressings are known to mediate successful wound recovery [27]. This is usually achieved through repetitive applications of medicament, and frequent dressing changes. However, the process on the whole is inconvenient and painful. Frequent visits to medical centers or hospitals are required to fulfill multiple drug dosing requirements as well.

In many formulations, an initial large dose of drug is released as a bolus dose when the drug comes in contact with the release medium. Thus a burst release phenomenon is observed, which also reduces the lifetime of the drug delivery device. One of the complications of burst release is that it is difficult to control and is unpredictable [28]. However an initial burst release has the effect of providing initial relief, followed by a sustained release profile[6]. In spite of this, in vivo drug concentrations after burst release may reach toxic levels, raising therapeutic and economical concerns [29].

Stringent efforts have been made in the past to optimize drug release so that a locally sustained or controlled release pharmacokinetic profile may be attained through transdermal drug permeation instead of through the more common systemic route [30]. In chronic wound therapy, controlled drug release from a bandage ensures consistent and sustained delivery of medication to the injured site, at the same time obviating the need for frequent dressing changes [31]. In such cases, peak and valley drug profiles are avoided, and drugs with shorter half lives can be delivered. These effects may contribute to improving patient compliance with the treatment regimens and by design improving treatment prognosis as well [32]. Polymeric materials are particularly useful in the fabrication of bandages where it is necessary to avoid high systemic doses of antibiotics, while treating the infected wound site with localized concentrations of antibiotics [33][34].

The necessity of optimizing controlled release formulations for treatment of disease arises from the therapeutic requisite to reduce the amount of drug concentration needed to produce desired effects in patients [35]. Targeted or controlled release therapy also improves patient compliance, because of easier dose regimens and the diminished requirement of multiple dosing [36].

To achieve targeted drug release profiles from novel wound dressings, a dual spinneret electrospinning technique has been used in which two drug are used simultaneously, where it was found that the use of two drugs simultaneously in one matrix changed the release profile of one of the drugs [37]. Transdermal Drug Delivery systems have also employed piezoelectric materials to control the delivery of drugs [38].

Advancements in the field of auxetic biomaterials however, may pave the way for more convenient possibilities in the field of controlled drug delivery. Auxetic materials have a negative Poisson's ratio, that is, they increase in cross section in the directions parallel and perpendicular to the direction of applied load [39][40]. Thus for an auxetic material with a porous morphology, an increase in pore size will take place in response to uni-axial loading. This will also be associated with a large volume change. These properties have been explored with reference to auxetic materials acting as molecular sieves, entrapping a particle and then freeing it in response to pore size changes after directional loading. Such characteristics have the potential to be harnessed for use in fine tuning the release of drug from a matrix system [33].

Phase I - A Macro-Scale Model of a Tunable Drug Dispensation Device for Enhanced Wound Healing

This research has been divided into two phases; in the first phase, the ability of auxetic polymeric films with regards to retaining or controlling the release of particulate matter (in response to actuation through an externally controlled mechanism) has been explored; all aspects of the fabricated device have been explored with pertinence to controlled drug delivery for wound healing. Thus the proposed device is expected to be an externally worn contraption. A macro model assembly for possible use in enhanced wound healing and controlled drug delivery applications has been presented here. The macro model assembly

presented comprises of an auxetic film, and a mechanism with drug reservoir contained between the two opposing interfaces. All of the components of the assembly are arranged in laminar fashion, with the auxetic film and the mechanism conjugated at the ends. Because of this, any extension in the mechanism will ultimately cause extension in the auxetic film, changing pore size, and allowing drug particles to pass through. The amount and rate of drug particles that pass through the film may be controlled by actuation of the mechanism at the lever ends (see Figure1). The prototype presented here has adjustable porosity for fine tuning the amount of drug dispensed to a wound during chronic wound healing.

It would be pertinent to mention that the model depicted in Phase I of this study does not compensate for the aspect of exudate removal in chronic wounds. The control over drug delivery is manual, so there might be possible challenges related to the accuracy of the amounts of drug delivered. To overcome these limitations, a miniaturized version of the model with additional features, was conceived, designed and fabricated. This constitutes Phase II of the study.

Phase II - Electromechanically Actuated Multifunctional Wireless Auxetic Device for Wound Management

In Phase II of the study, we present a novel design for a miniaturized version of the device detailed earlier; this device has several additional features. It houses an auxetic component that is actuated by electronic means to help strictly regulate the amount of medicament that reaches the site of the wound (Figure 3 a and b). The miniaturized version of the wound healing device has been modified to include an electronically actuated drug delivery mechanism and also includes a provision for exudate removal during treatment of chronic wounds; this device embraces the concept of holistic wound management, obviating the need for frequent hospital visits or painful dressing changes.

Literature Review:

Wounds are of a variety of types and each category has its own distinctive healing requirements. This realization has spurred the development of a myriad of wound dressings, each with specific characteristics. It is unrealistic to expect a singular dressing to embrace all characteristics that would fulfill generic needs for wound healing. However, each dressing may approach the ideal requirements by deviating from the 'one size fits all approach', if it conforms strictly to the specifications of wound and the patient. Of course a functional wound dressing would be expected to achieve healing of the wound with minimal time and cost expenditures. The current article offers insight into several different types of dressings in clinical use, the materials specified for these dressings and the events taking place at cellular level which aid the process of healing while the biomaterial dressing interacts with the body tissue. Hence the significance of using Synthetic Polymer Films, Foam dressings, Hydrocolloids, Alginate dressings and Hydrogels have been reviewed, and the properties of these materials that conform to wound healing requirements have been explored. The role of bioactive dressings that play an active part as healing as well as drug delivery agents has been reinvestigated. A special section on Engineered Skin Substitutes as part of the advancement in this area of novel clinical treatments has also been considered.

For effective wound healing to occur there has always existed a requirement for a suitable material that would cover the wound to prevent infection [1]. Biopolymers, materials such as animal fats, plant fibers, and honey pastes were commonly used in the past as wound dressings [2]. A few years later dressings like cotton wool, lint and gauzes started being used as dressings, and their main function was to keep the wound dry by allowing wound exudates to evaporate and by inhibiting invasion of bacteria from the surrounding environment [2]. Recent studies have proven that a moist and warm environment provides a better alternative to previous wound healing therapies. The compatibility of the physical and chemical properties of the dressing with the nature of the wound must be taken into account when designing a bandage for wound healing. An active wound dressing controls the biochemical state of the wound in order to aid the healing process. No wound dressing is ideal, but the minimum requirements of rapid healing, affordable cost to the patient, aesthetics and prevention of infection must be fulfilled during wound management [3].

Physiology of wound healing:

Wounds are an unnatural break, tear or defect in the skin, caused by thermal/physical injury, or an underlying pathological condition [4]. Based on the repair process wounds may be classified as acute or chronic wounds. Acute wounds are tissue injuries mostly which tend to heal completely, usually within a time frame of 8-12 weeks and with minimal scarring. Chronic wounds generally tend to reoccur and have a healing time extending beyond 12 weeks [5]. Underlying physiological conditions may result in delayed healing of a wound, or complete failure of a wound to heal. Bedsores and leg ulcers [ischemic or venous] are examples of chronic wounds [6].

Skin layers and affected area are also used as basis for classification of wounds. Superficial wounds are those that involve only the epidermal skin surface. Injuries that involve the epidermis, deeper dermal layers, blood vessels, sweat glands and hair follicles are known as partial thickness wound. Full thickness wounds are caused when the subcutaneous fat or deeper tissue along with the epidermis and dermal layers is injured. [7, 8].

The process of wound healing comprises several stages, namely hemostasis, inflammation, migration, proliferation and maturation [9].

Hemostasis is initiated by clotting factors in the wound exudate. When a wound bleeds, it automatically performs the function of flushing bacteria and/or antigens from the infected/damaged tissue site. Fibrinogen mediates the clotting action by forming a fibrin network and this produces a clot in the wound which stops the bleeding. When the clot dries up it forms a scab, which helps in supporting and strengthening the weakened tissue [10]. The inflammatory phase consists of both cellular and vascular responses. Vasodilatation caused by raised levels of histamine and serotonin allows phagocytes to enter and engulf dead cells. Hard necrotic tissue is liquefied by enzymatic action and assumes a yellowish appearance. This is commonly called 'Sloughy'. Platelets from the damaged blood vessels form aggregates during the clotting mechanism. The Migration phase involves the movement of epithelial cells and fibroblasts to the injured area to replace tissue. Cell regeneration then occurs rapidly over the wound under the dried scab, along with epithelial thickening [9].

Cell proliferation occurs almost immediately or just after migration phase and might last for 2 or 3 days. Granulated tissue known as 'Stroma' is formed in about 4 days by the internal growth of capillaries and lymphatic vessels inside the wound. Collagen synthesis occurs due to fibroblasts, giving the skin strength and form.

Formation of blood vessel and granulation tissue is completed to its maximum level by the fifth day. More epithelial thickening occurs until the wound is bridged by collagen.

Fibroblast proliferation and collagen synthesis continues for around 2 weeks until the edema recedes. The maturation phase brings about the formation of cellular connective tissue and strengthens the new epithelium which shapes the nature of the final scar [11]. Excess wound exudate can lead to complications. However, studies suggest that exudate resulting from acute wounds may actually aid the wound healing process, while in chronic wounds it may inhibit wound healing [12].

Chronic wound healing is a result of disruption of the normal sequence of wound healing events. In such a case the primary concern should be that all possible sources of infection are cordoned off. Excess exudate should be controlled and foreign bodies should be removed. Closure of the wound should not occur too early, especially in case of infected wounds [13].

Occlusive/Polymeric dressings used for wound healing:

It is a widely accepted hypothesis that moist wound dressings promote a faster rate of wound healing as compared to dry wound dressings. This hypothesis was put to test through Winter's experiments who showed that epithelialization occurred twice as fast in young domestic pigs with moist wound dressings as compared to those with a dry wound dressing. Scab formation was also prevented in moist wound conditions [14].

Subsequent studies on dermal wound healing have taken into account the proliferating rates of cellular entities involved in wound healing. Comparing the effects of moist and dry wound conditions affecting the populations of both kinds of cells it has been found that inflammatory phase cells [neutrophils and macrophages] failed to multiply rapidly in a moist wound environment. Whereas the numbers of endothelial and fibroblast cells increased in moist wound conditions as compared to wounds that were kept dry [15].

Movement of epithelial cells across wound surfaces is facilitated in wounds that are kept moist and scab free. This in turn promotes wound healing [16]. Superficial wounds are susceptible to pronounced scar formation in some individuals. Wounds that are kept moist are prone to less obvious scab formation, thus alleviating cosmetic concerns [17,18]. Reduction in pain symptoms of patients has been observed in moist wound healing environments [19].

Occlusive dressings that are now commonly used act by keeping the wound sealed so that moisture is trapped in the wound. Thus the wound is also kept safe from desiccation and further tissue damage from exposure to the environment. As explained earlier, desiccation and trauma hinder the migration of epithelial cells toward the damaged site [20]. Since epithelial cells have a key role in wound healing, this parameter should be kept in consideration when designing a dressing to cover the wound.

Prevention of wound desiccation results in the formation of an electrical potential between the moist environment of the wounded tissue and the drier area of the non wounded surrounding tissue. This stimulates the migration of epithelial cells towards the wound site. Expression of growth factors on fibroblast cells also increases after providing electrical stimuli. Both these factors aid wound healing [21, 22]. Occlusive dressings are costly but have been shown to give effective results in treatment of wounds with shorter nursing period [3]

Synthetic Polymer Films as wound dressings:

Polymer films were initially introduced as drapes for surgical incisions. However later they have now carved a niche in wound healing management as occlusive dressings. Polymer films trap exudates, hence providing a moist environment for wounds. One main feature is that these films are impermeable to bacteria and liquid but are permeable to moisture vapor and air. Exudates from wounds may accumulate underneath the film since these dressings are non absorbent. Although this does not appear to encourage bacterial growth in the wound, the seeping fluid pressure may cause a break in the environment maintained by the occlusive dressing.

Synthetic polyurethane films have been analyzed as potential polymeric wound dressings. As compared to the control dressing, wounds covered with polyurethane films formed a thinner scab, with lower inflammatory cell infiltration. The studies also showed earlier formation of granulation tissue on the wound site, which was vascularized and rich with collagen. Wound healing also depicted a better rate of epithelial cell organization as compared to the control [23].

A wound dressing thus approaching ideal characteristics should conform to the site of the wound, offer alleviation of pain symptoms, promote faster wound healing time and attempt to restore the patients normal daily activities. This review of literature highlights the need for a more holistic approach towards wound healing and management so that while selecting the appropriate dressing for a wound, the physiological and biochemical requirement of the wound and the patient are also taken into account.

Materials and Methods (Phase I):

For the macro-model design Polyurethane (PU) was the material selected for the fabrication of the auxetic film underlying the mechanism for drug delivery control. PU was chosen because of its excellent biocompatibility, and suitable machining characteristics. PU films may also be tailored according to the application, by permutation of hard and soft segment ratios. The design used for fabrication of the auxetic film is based on the rotating squares model [39]. The behavior of this design may be mapped out on the basis of both the angles formed at the vertices where the rotating squares join, as well as by the hinging and stretching constants. In addition to these parameters, the direction in which force is applied also plays a role in the stretching characteristics of the film. All of these parameters have been explored with particular reference to the scissor mechanism that controls the stretching behavior of the film. It would be pertinent to note that the mechanism simultaneously limits the stretching behavior of the film and hence the porosity which controls drug elution.

Casting of Polyurethane Film:

The Polyurethane used was PMC-744, of hardness 44 Shore 'A' (supplied by Smooth-On Inc.PA, USA). The two part (A and B) polyurethane was mixed in the ratio of 2A: 1B and then poured over the ABS plastic mould. The standard 18 hour curing period was followed for film casting, after which the film was peeled off the mould and left for another 24 hours in air to achieve full curing.

Manufacture of Mould through Fused Deposition Modeling:

The mould for polymer casting was prepared through additive manufacturing technique, FDM (STRATASYS FDM 360mc machine). The parts extruded through FDM were based on thermoplastic acrylonitrile-butadiene-styrene (ABS). The 3-D model of the negative replica of rotating square geometry was first designed through PRO/Engineer version Wildfire 5.0. Based on the computer generated model, the mould was then fabricated by the FDM machine using ABS plastic as the modeling material.

Manufacture of Bandage mechanism by Stereolithography:

The mechanism that controls the pore size of the auxetic film has been manufactured by SLA (stereolithography technique). In this technique a CAD design of the mechanism model was first converted into STL format. Rapid prototyping of the mechanism was carried out based on the given STL format.

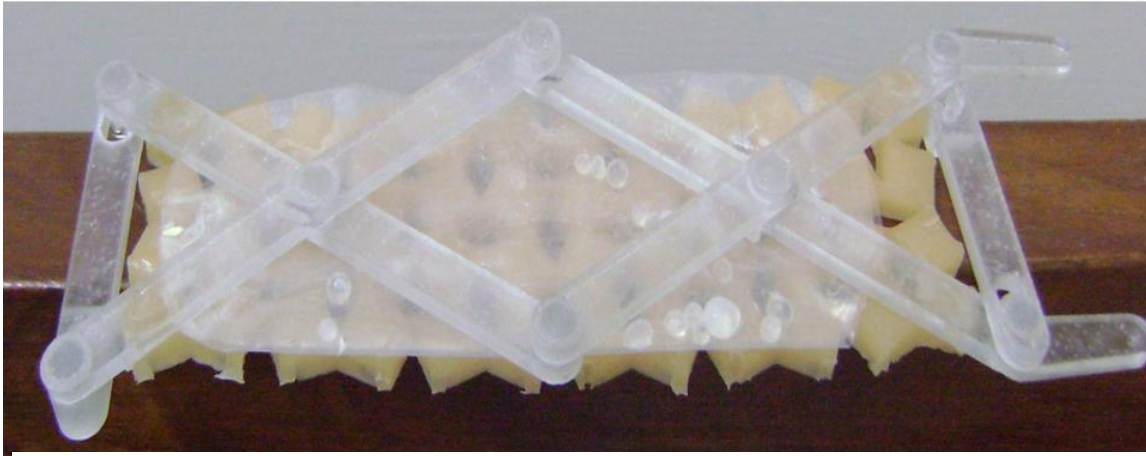


Figure 1. Showing a macro model of the mechanism, drug reservoir and auxetic film in laminate arrangement

The mechanism assembly comprises of 14 components, which includes 6 bars and 8 pins, which allow the bars to connect and move with reference to each other. Each part was manufactured separately and then assembled to form a functional mechanism; refer to Figure 2b. The mechanism functions with a number of elongated bars that are interlocked with pins. The arrangement of the bars is such that they operate through a scissor like mechanism. The basic operation depends on the fact that if force is exerted in the 'x' direction Figure 2a, mechanism extension will take place along the 'y' direction. The overall extension of the mechanism is limited by the size of the slits that hold 4 of the pins at the extreme ends of the assembly.

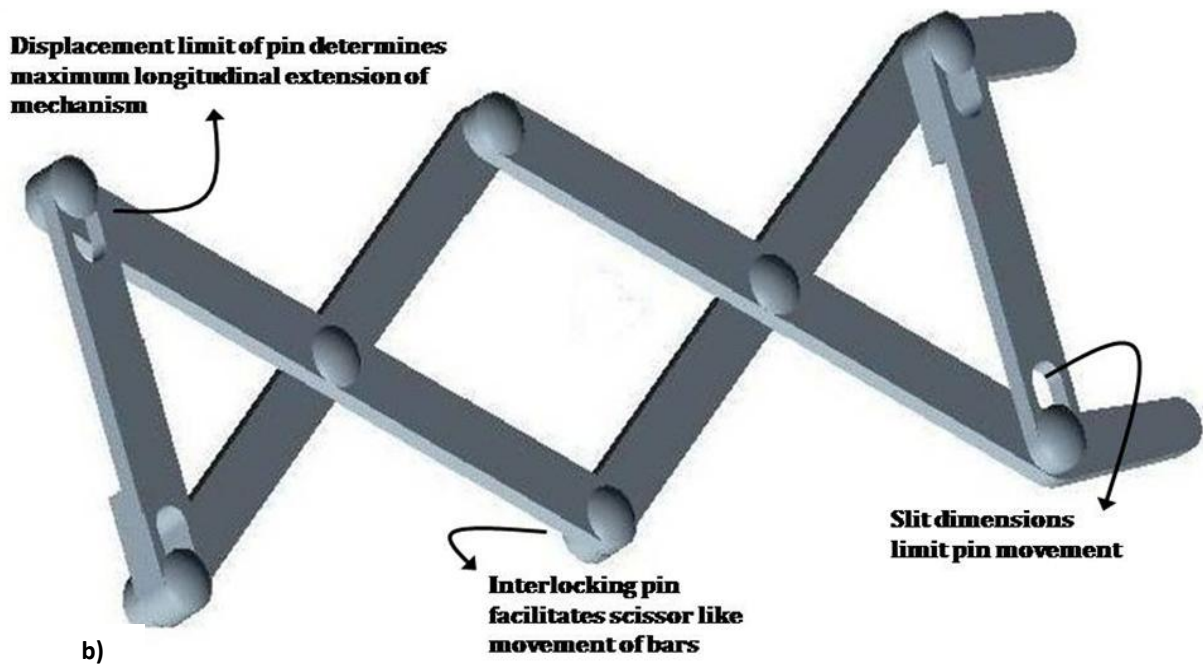
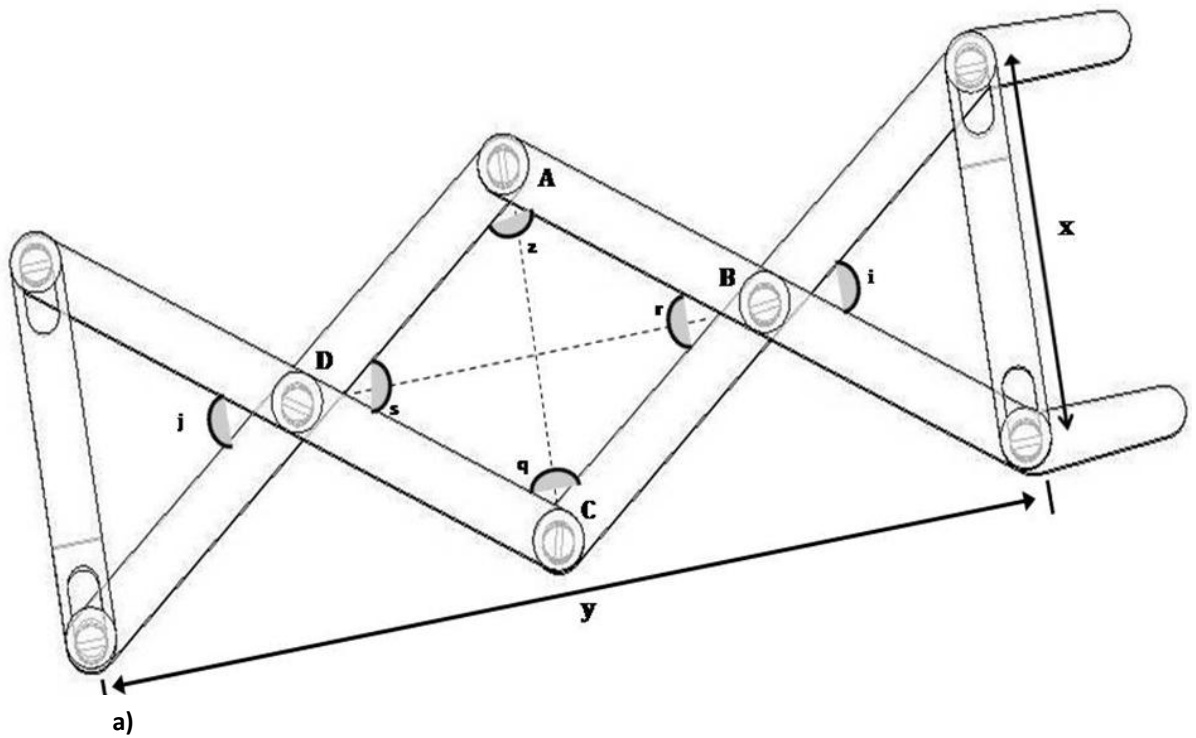
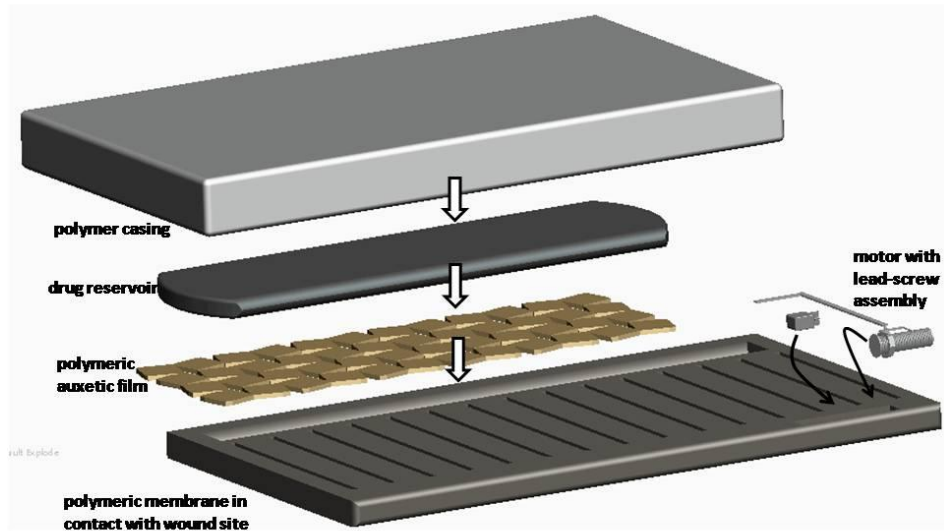


Figure 2 a) The figure shows the angles that change during mechanism extension and direction of extension (y) as well as direction of actuation (x) of the mechanism; b) schematic shows interlocking pins and slit width that permits and limits extension of the mechanism.

3.0 Characterization of film extension through Image Processing:

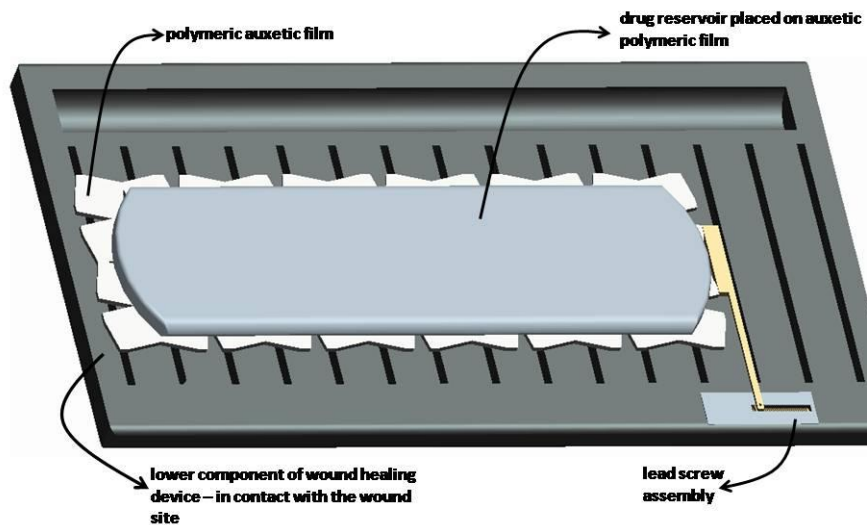
The auxetic film behavior was characterized through the image processing software in MATLAB, (R 2009 b). Measurements of the extended and un-extended film were recorded through images taken with a Digital Camera (SONY, DSC-S 750, China), and characterized after scaling the pixel to centimeters ratio with the image processing toolbox in MATLAB. The images were taken from a fixed distance of 25 cm, so that all images correspond to the same pixel: centimeter ratio. This was facilitated by the construction of a bridge set-up, in which the camera lens fits through the aperture, and the film is laid out underneath. The pixel to centimeter scale for these images was found to be 37.8:1. Subsequent calculations of film extension were carried out using this scale. Time lapse images of the drug particle being released from expanded pores in the auxetic film were also taken with Nikon D 3100 camera (see Figure 12).

Materials and Methods (Phase II):



a)

Laminate arrangement of wound healing device components



b)

Figure 3 a) Showing laminate arrangement of all components within the device, b) Skin surface component in contact with the auxetic film which is placed beneath the drug reservoir

Design of the Device and its components:

CAD designs of all device components were modeled in Pro E wildfire version 5.0. The device has been designed so that it has a laminate structural arrangement of six individual components that work in synchrony to perform dual functions of taking up wound exudate and administering controlled doses of drug to the wound site. The first component, which will come directly in contact with the skin, has a number of recessed features (the skin facing surface of the device). The recessed features or grooves (figure 4), are designed so as to house absorbent material. These grooves are connected by miniscule channels to a main conduit (on the posterior surface), that will also be filled with absorbent material. The skin surface component also has a number of hollow slits that will allow the drug to reach the wound site. These hollow slits are in direct contact with an auxetic polymeric film (Figure 3a) which is placed directly underneath the drug reservoir.

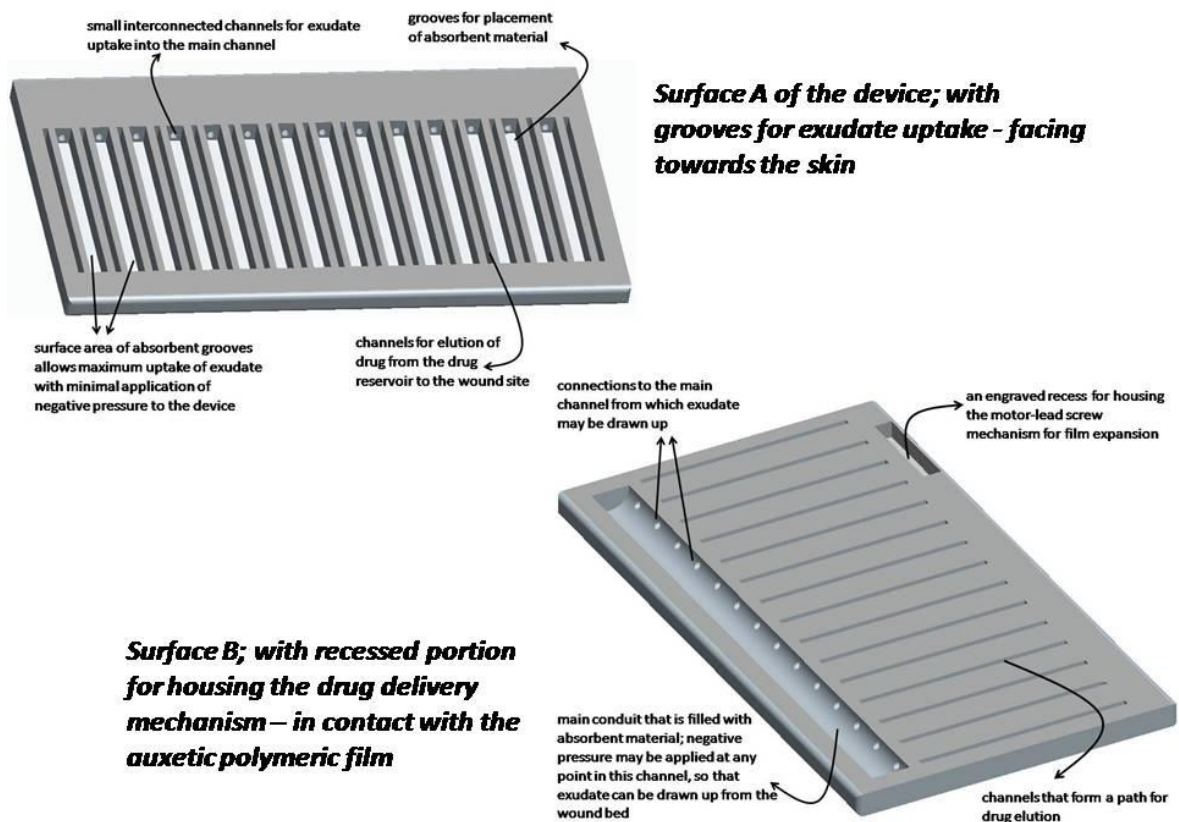


Figure 4. Showing CAD model; features in surface A (skin contacting surface), and surface B (in contact with the auxetic film)

This laminate arrangement allows the auxetic film to act as a barrier that can effectively limit the rate of drug administration to the wound site. Film expansion (and in turn expansion of the film pores), can be actuated through electronically controlled mechanisms, two of which have been explored in this study. The design of the auxetic film facilitates this event, because each unit cell is a planar structure of four connected squares rotated at an angle to each other and forming a diamond shaped hollow space between them; a connection between the two unit cells in both vertical and horizontal directions form hinges; the entire auxetic structure comprises of a repetition of such unit cells patterned vertically and horizontally. The auxetic rotating squares design [39] of the polymeric film allows it to expand in both parallel and perpendicular directions in response to a uni-axial application of force, thereby leading to an overall increase in pore size (Figure 5).

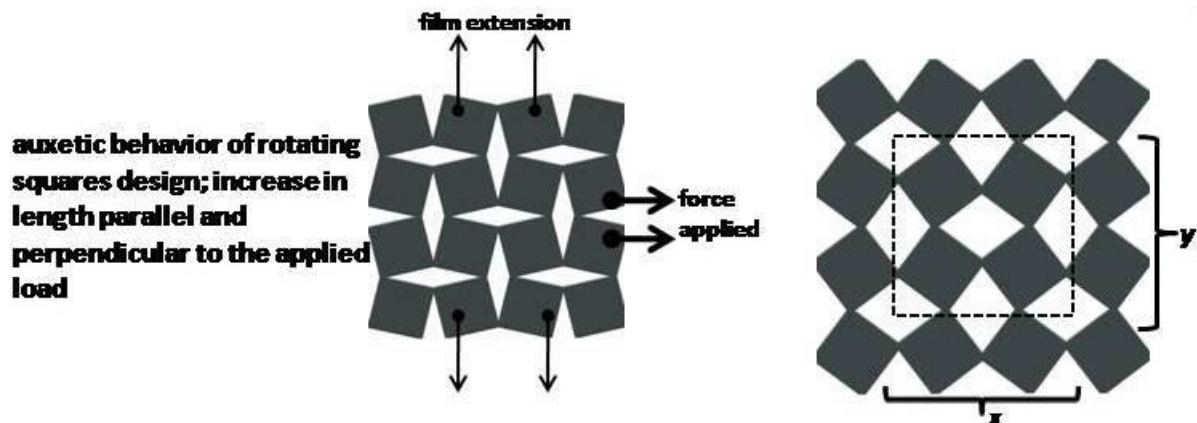


Figure 5: Showing auxetic behavior of the rotating squares design

In this work, two mechanisms have been explored with reference to film actuation. The first mechanism is a string-pulley mechanism. This mechanism acts through the transmission of force across a string that is attached at one end to the auxetic polymeric film and from the other end to the rotating shaft (motor head); refer to Figure 6a. This mechanism is based on the concept of a simple fixed pulley system; in this case the axle is a relatively frictionless surface (a fixture on surface B of the device), which acts as a circumference along which the string moves. The main purpose of this additional fixed structure was to cause a change in the direction of force transmitted along the string, so that the direction of the pulling force

acting directly on the auxetic film is completely horizontal. Since one end of the string is attached to the rotating shaft of the motor head, when the shaft rotates in either clockwise or anticlockwise direction, the string gets wound circumferentially on the motor shaft, thus getting tighter; the force in the taut string is transmitted through to the auxetic film, which expands in response.

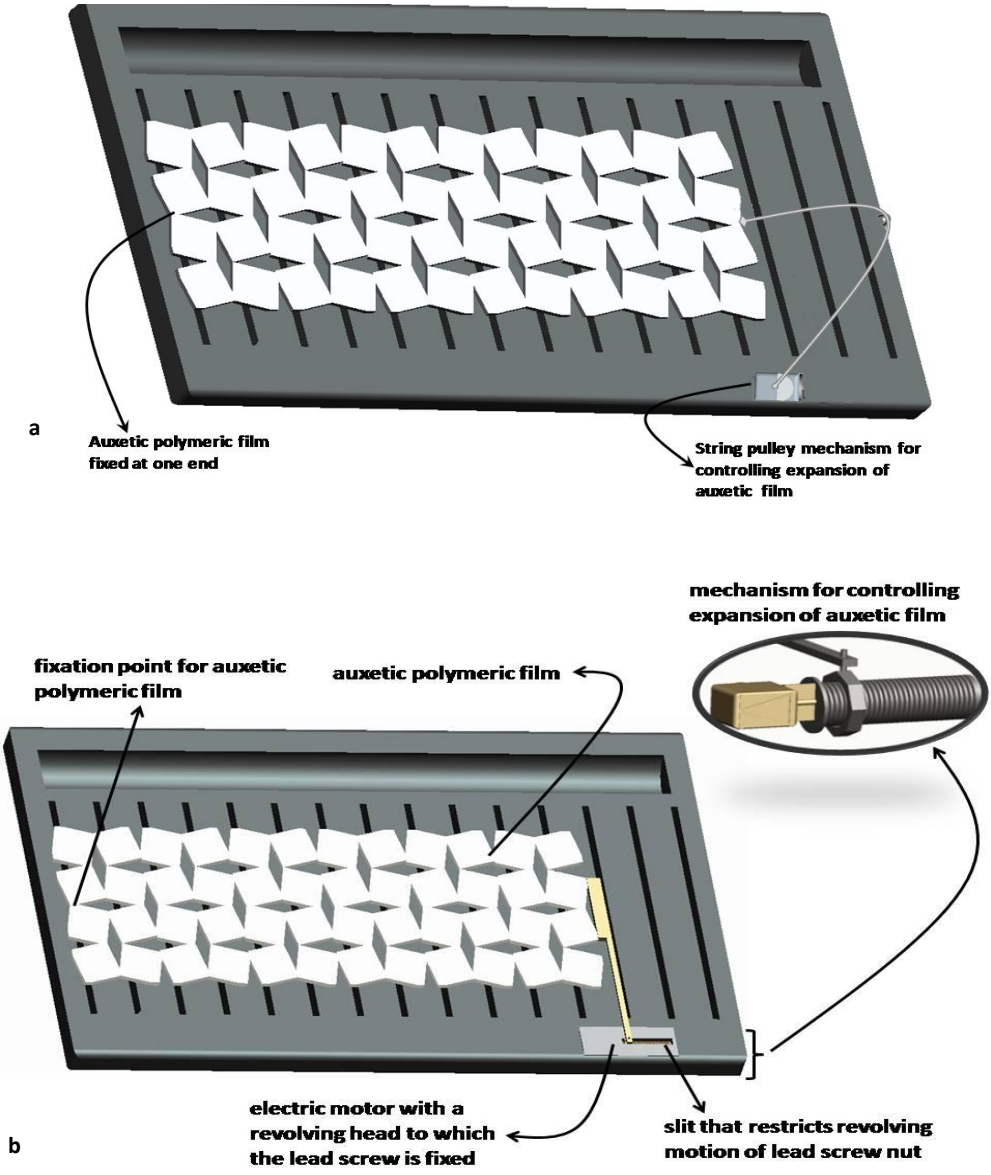


Figure 6: a) Showing schematic of the pulley mechanism, b) CAD model of the lead-screw mechanism

The second mechanism employed for controlling drug delivery is the lead screw mechanism. Like the pulley mechanism explained earlier, this mechanism controls the expansion of the diamond shaped pores in the auxetic film. Ultimately, this modulates the amount of drug that is eluted through auxetic film and the polymeric skin surface component of the device to reach the wound site. Figures 6b shows that the auxetic film extension is caused because of linear forward motion by the lead screw nut, which is connected to the auxetic film through a beam attachment. This linear motion is controlled by rotation of the revolving motor head (shaft – refer to figure 6b), which is attached to the lead screw. The rotation of the lead screw nut is restricted by the protruding pin on the nut surface; this pin goes through a slit that is part of a covering for the entire recess where the mechanism is accommodated. Because rotating motion of the nut is restricted by this slit, the only motion that the nut is allowed is forward and backward linear motion, in response to rotation of the threaded screw. This rotation takes place in response to rotation of the motor shaft head, which is connected to one end of the threaded screw (refer to figure 6b). This linear motion of the nut and hence the beam to which the film is attached, is translated into force that acts on the auxetic film, so that the pores can be opened or closed in response to linear forward or backward motion of the lead screw nut and beam. Since pore expansion is controlled through this mechanism, the amount of drug that elutes through the auxetic film can be controlled.

Fabrication:

The main structure of the device (skin surface component and the auxetic rotating squares film) was fabricated using Polyurethane (PU) PMC-744, of hardness 44 Shore ‘A’ (supplied by Smooth-On Inc.PA, USA). Polyurethane was chosen because of its excellent machining characteristics and in particular for this application, a PU of this hardness (44 Shore A) was chosen because of its suitable elastic properties.

Auxetic Polyurethane Film:

For fabrication of the auxetic Polyurethane (PU) film, commercially available Parts A and B were mixed in the ratio (2A:1B), and casted on a level surface, at a thickness of 0.5 mm.

A standard curing time of 18 hours was followed, after which a PU film was obtained. A CAD design of the rotating squares film (described above), was imported into the Laser/Cut-Engrave software. Laser cutting equipment Shenzhen Lead CNC-LS240A was used, and the process was carried out at Power 20 W, Speed 20 mm s⁻¹.

Structural components of the Device:

Fabrication of the device structural components was also carried out through the laser cutting process. PU was casted (thickness 4 mm) and cured at standard curing time before laser processing. Both cutting and engraving features were used for the skin surface component (Surface A and B). Parameters were modified to account for the different thickness of this polymer cast. Laser cutting was carried out at a Power 20W and Speed 2 mm s⁻¹; laser engraving (for formation of grooved features) was carried out at a Power 50 W, Speed 200 mm s⁻¹ and a step size of 0.05 mm. The casing for the device was also imported from a CAD design into the software and then fabricated accordingly.

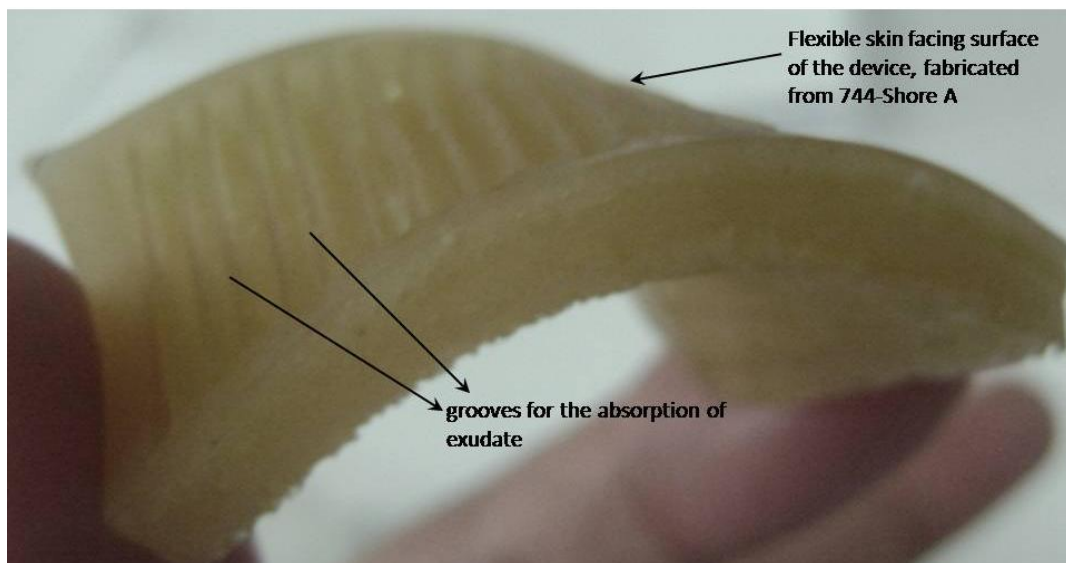


Figure 7: showing the flexible skin facing surface of the device, fabricated from Polyurethane 744, Shore A

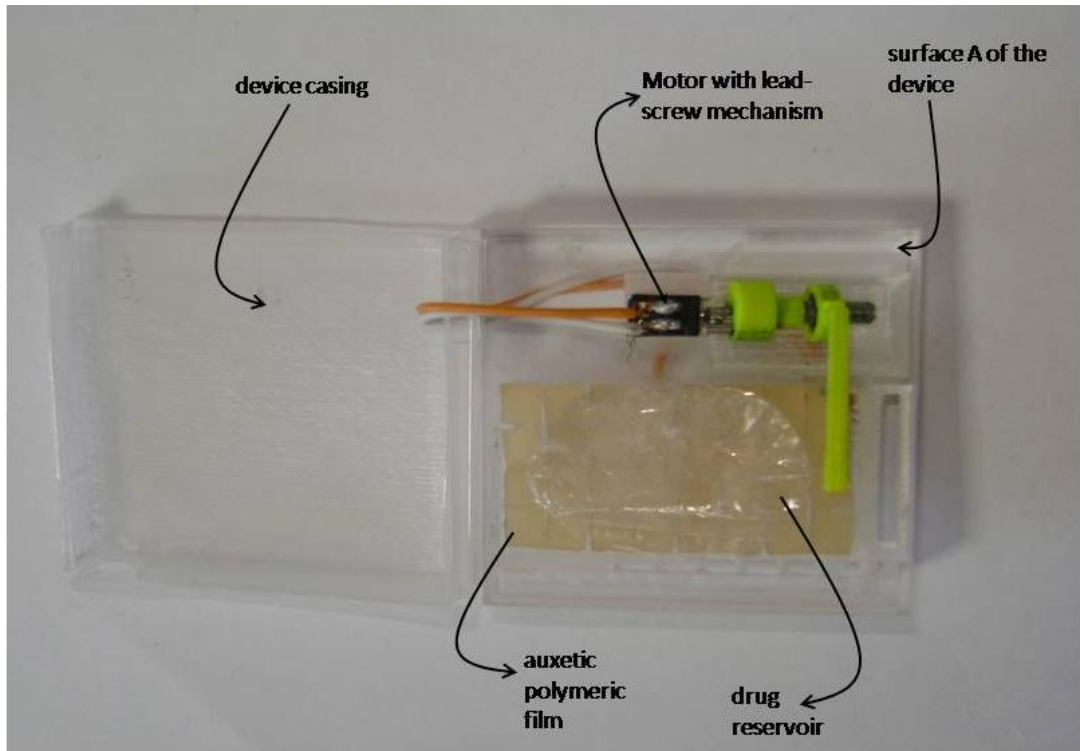


Figure 8: Showing laminate arrangement of the fabricated device with the auxetic polymeric film actuation controlling mechanism and the drug reservoir

Circuitry for Pulley and Lead Screw Mechanisms

Both mechanisms are voltage driven, the optimal operating requirement was found to be 3 Volts and 0.17 Amperes for the pulley mechanism. The lead screw mechanism had to be configured with NPN transistors in an H-bridge configuration circuit, to satisfy the same voltage requirements without the use of a higher battery voltage. An Arduino Mega 2560 microcontroller was used to support device function for both mechanisms.

Test Methods used for verification of device functions:

Drug Delivery:

This novel multifunctional wound healing device design was tested for drug delivery and exudate removal functions. The testing frame developed for this purpose was an acrylic

prototype of the device that has exactly the same structural components, but an additional provisional feature for collection of drug that passes through the auxetic film and through the cut out slits; after each reading, the exact amount of drug eluted was collected at the bottom of the test bed. To represent the powder medicament that elutes through the auxetic film pores, a pharmaceutical diluent Lactose-D-Monohydrate (Sigma Aldrich, Germany), was used. The amount of medicament was weighed, and recorded for each film actuation reading. As stated earlier, both mechanisms were used in tandem with a microcontroller; this allowed the motor to be powered for time intervals ranging from less than a 100 milliseconds to more than 300 milliseconds. This time interval directly corresponds to the number of times that the motor shaft rotates (in either clockwise or anticlockwise directions according to the polarity of the motor terminals). An increased time interval (and hence an increased number of shaft rotations) means a higher degree of film extension and greater opening of pores in the film. Weight recordings have been made with ten such time intervals ranging from 75 milliseconds to 325 milliseconds. A 25 millisecond gap separates each recording. A total of ten sample readings have been recorded, and each reading has been repeated five times to determine the reproducibility of the amount of drug eluted through standard deviation calculations.

Exudate Removal:

The quantity and ease of exudate removal from the device was assessed through using a simulated wound exudate solution (sodium chloride/calcium chloride solution with 142 mmol sodium ions and 2.5 mmol calcium ions). Exudate removal tests were performed using cellulose fiber as the main absorbent material in the grooves (Surface A) and the main conduit (Surface B). The simulated wound exudate is drawn up from the device by applying minimal negative pressure to an access point in the casing of the device that goes through to the main conduit. For each reading, the simulated wound bed was refilled with 2ml of the ionic solution (exudate). Thus active purulent wound conditions were simulated.

Results (Phase I):

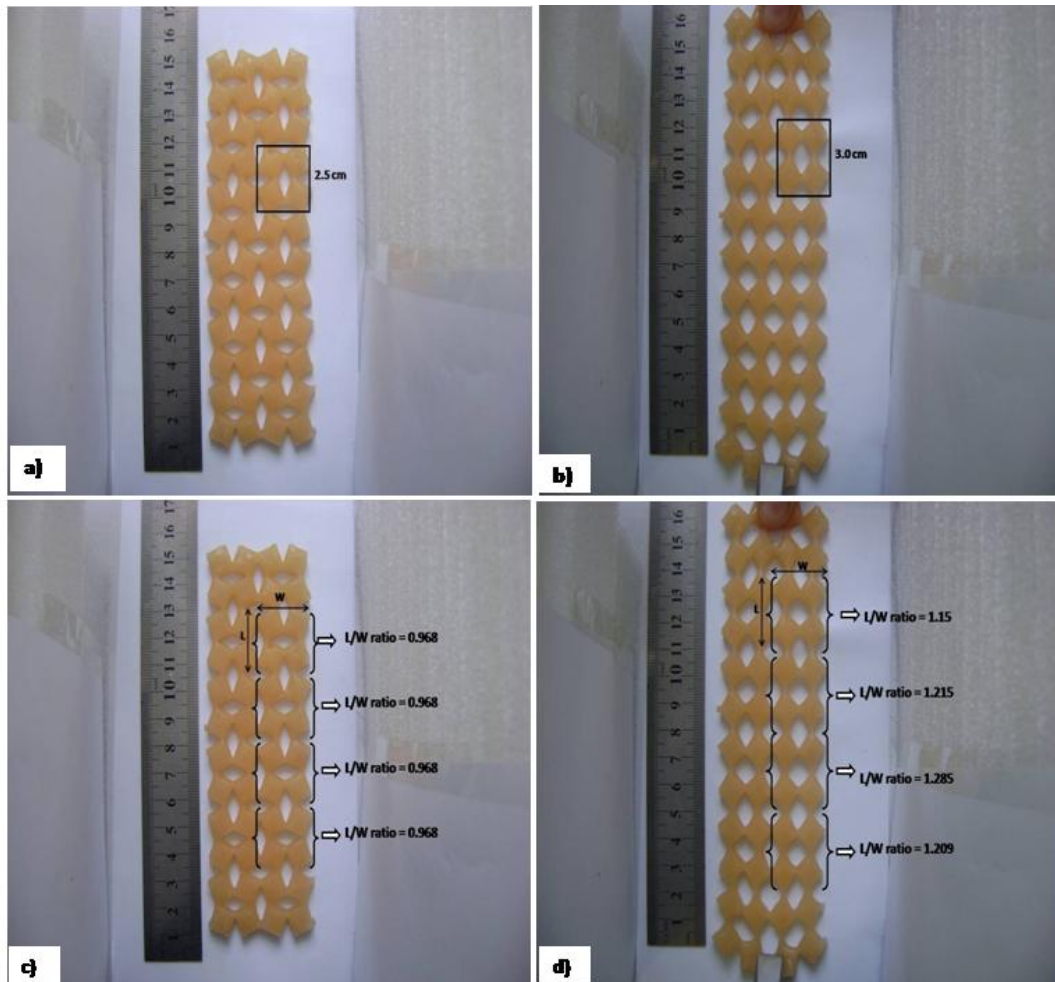


Figure 9 a) The dimensions of one unit cell in the un-extended film are shown, b) The change in dimensions of the extended unit cell are highlighted, c) L/W ratios of the un-extended film are shown, d) L/W ratio of the unit cells in the film when it is in extended form.

Figure 9 shows images of the original (un-extended) and extended auxetic film. One unit cell in the original film (shown in figure 9a), measures 2.5 cm, while measurements for the same unit cell in stretched condition go up to 3.0 cm. It is evident from the processed images that a maximum extension of 0.5 centimeters is possible. As shown in Figure 3, the Length to Width ratios of the four unit cells range from 1.15 to 1.215, 1.285 and ultimately 1.209. The increase in length of each unit cell of the auxetic film is greater than the increase in

width, although a two dimensional increase does take place, in both 'x' and 'y' directions. As discussed earlier, this extension is subject to minor variation throughout the film. However, since the film is constrained (for stretching) from both extremes, the unit cells on both extremes (that is the first and sixth unit cell) are not taken into consideration when measuring maximum extension of the film.

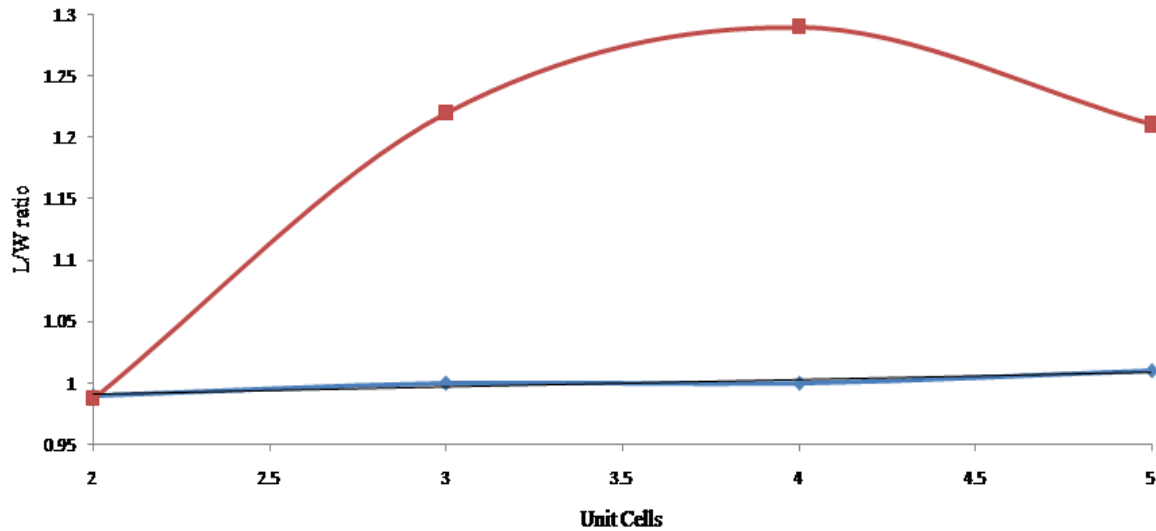


Figure 10. Graph showing the parabolic pattern that the extended auxetic unit cells follow. As is apparent from the graph, the third and 4th unit cells (middle region of the film) show more expansion than the rest.

The ratio measurements, Length/Width (L/W) throughout the length of the film may be patterned out as a parabolic curve, as shown in Figure 4. In contrast to this behavior, the L/W ratios of all unit cells in the un-extended film follow a relatively linear graph. The curve shown in Figure 10 is significant because even though an equal amount of force is applied in at both ends of the film there is a greater expansion observed in the third and fourth unit cells as compared to the second and fifth unit cell. These measurements advocate the hypothesis that at the micro-level, a greater amount of drug is likely to elute from this region of the bandage than at the extremes. This has been represented pictorially in Figure 11, below.

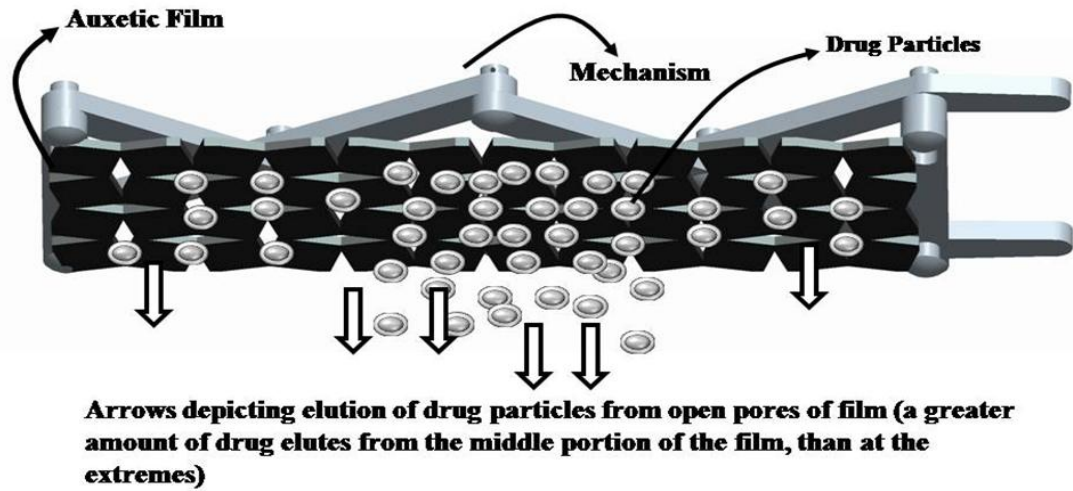


Figure 11. A schematic depicting drug elution from the bandage assembly, a greater amount of drug elutes from the middle region than at the extremes of the film.

Testing of the macro model:

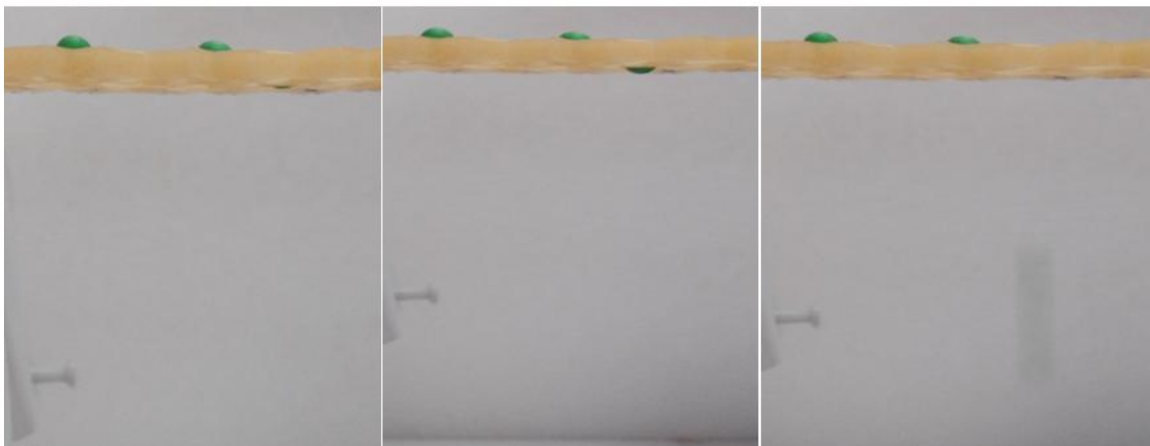


Figure 12. Images depicting the release of drug particles from expanded auxetic film pores.

As mentioned earlier, the extension of the film is controlled by the width of the slits at the extremes of the mechanism assembly. As the auxetic film is attached at both ends with corresponding ends of the mechanism, the stretching of the film is controlled by inward

flexion of the end levers of the mechanism (Figure 1 and 2a). Under a similar stress, a tear in a non auxetic (conventional material) would behave by becoming elongated in the direction of the force applied (or the axial direction) and by contracting in the transverse direction. In this case, if the dimensions of the tear increase in the axial direction, they decrease in the transverse direction, and thus there will be negligible increase in size, if at all. Hence if the film used in our study was replaced with a conventional polymeric material, the spherical balls that represent drug particles in this case, (see Figure 12) would not be able to pass through. However, because the film has an auxetic geometry, it will experience an expansion in the pore size in both transverse and axial direction, causing the pore size to increase, and thus allowing the passage of the drug particle through the pore. This phenomenon has been represented pictorially in Figure 12. The degree of expansion achieved, however, may still be controlled by the mechanism, and it is this property of the auxetic/drug reservoir/mechanism assembly, which may be utilized for adjustable drug delivery kinetics when tackling chronic infected wounds that require long treatment times and multiple doses.

In the model that we have created, the slit width of our mechanism allows for horizontal movement pins, which ultimately translates into a range of possible extension motions for the mechanism on the whole. Because the mechanism controls pore size in the auxetic film, the particle sizes that may pass through the film depend on firstly, the degree of extension of the mechanism and secondly on the slit width; which may be changed or modified in future models to accommodate a larger/different range of particle sizes which may be allowed to pass through the film.

The overall extension of the mechanism has been represented mathematically in ‘Mathematical Model 1’ given below. The condition depicting the range of particle sizes that may be allowed to pass through in the current scenario, have been explored in ‘Mathematical Model 2’.

Table 1

List of Notations used in Mathematical Model 1 and 2

Notation	Expanded Form
L_E	Extended length of auxetic film
L_0	Original length of auxetic film
N	Number of unit cells
X	Length of diamond arm
Dw_0	Original diamond width
Dl	Diamond length
Pd	Particle diameter

Table 1: Mathematical notations used in text

Mathematical Model 1:

The maximum extension that the auxetic film can achieve may be represented by the equation

$$L_E = L_0 + \sum_{n=1}^n n (x\sqrt{2} - Dw_0) \quad (1)$$

Where L_E refers to the extended length of the film, L_0 is the original length, n is the number of unit cells, x refers to the diamond arm, and Dw_0 is the original width of the diamond. Theoretically, substituting values into the expression $n (x\sqrt{2} - Dw_0)$ if n is taken as 1, then the total extension that the film is subject to is 0.5 cm. Practically this has been demonstrated when the number corresponds to the maximum change in length that is possible when the vertices of the diamond shaped hollow in one unit cell of the film are stretched out to form a square (refer to Figure 13 and Figure 14).

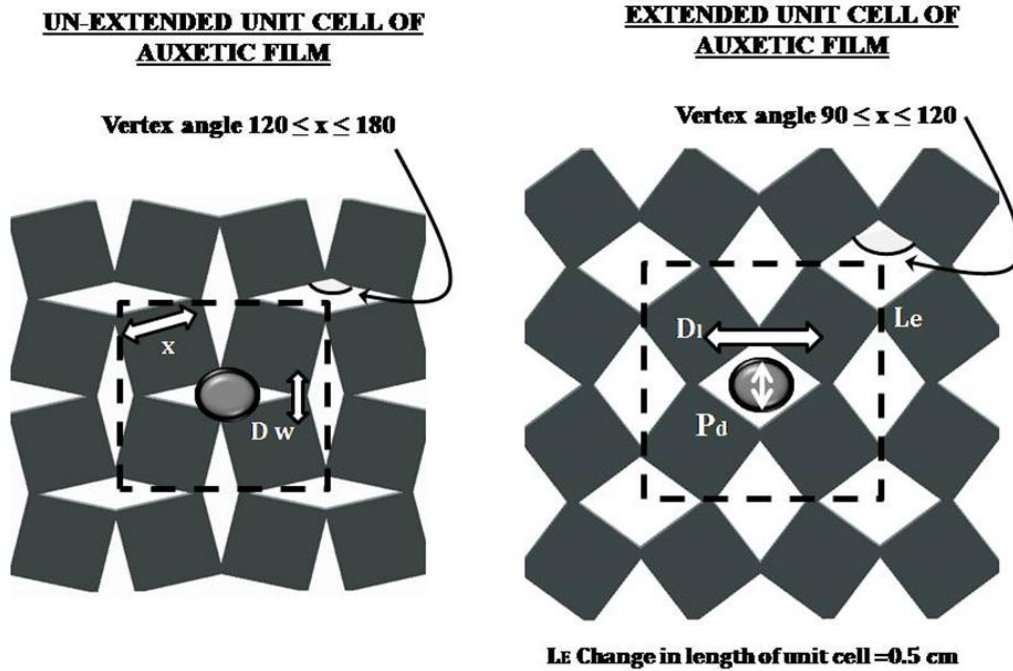


Figure 13. Figure showing the auxetic film in un-expanded and expanded form. As seen in the schematic, the drug particle with size 'Pd' is capable of passing through the diamond shaped pore when the range of angle is between 90° and 120°.

As shown in Figure 13, in the un-stretched film the Diamond length (Dl), is greater than diamond width, so that when the condition is $Dl > Dw$, the drug particle with diameter Pd, will not pass through the film. However when the film is stretched in one direction so that the diamond vertex angles move towards 90° the condition changes, that is the diamond changes toward a square formation. In this case, when Pd is less than both Dl and Dw, the condition " $Dl > Pd$, and $Dw > Pd$ " is satisfied, and the drug particle passes through the auxetic film. This change in pore size is controlled by manual actuation of the mechanism to which the film is attached, thus providing the advantage of adjustable porosity for controlled drug delivery.

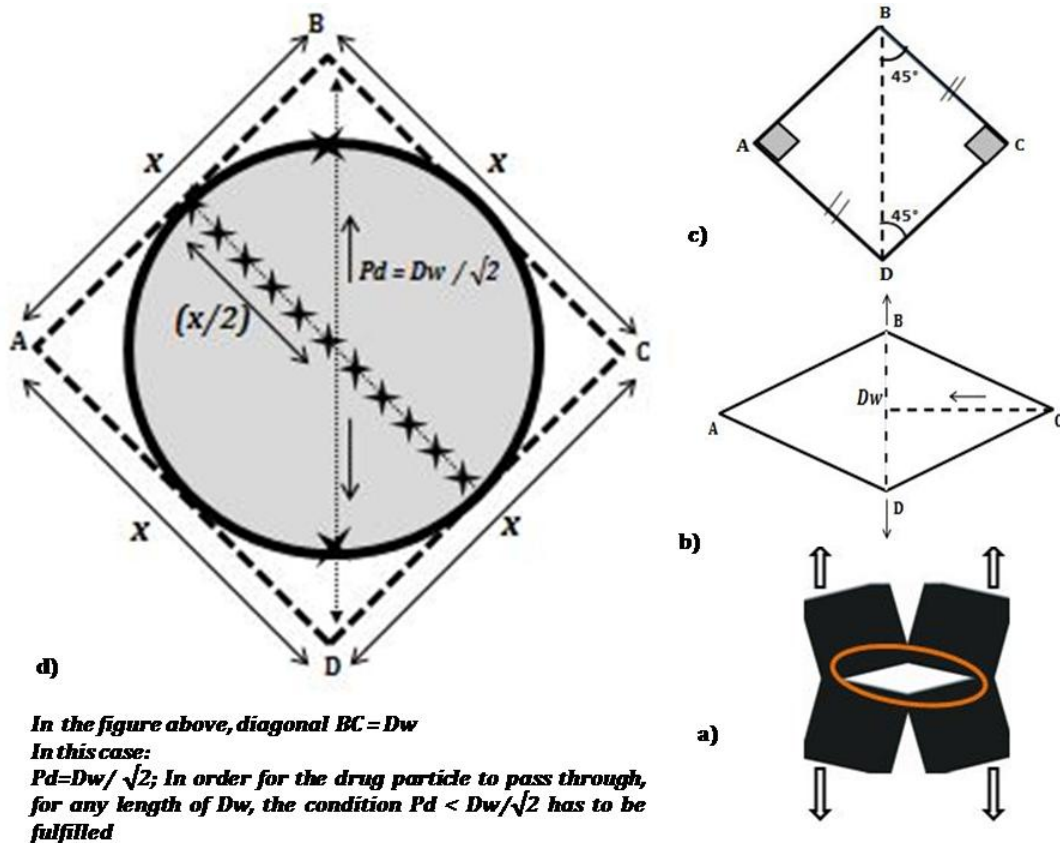


Figure 14. Schematic explaining mathematical model given below. The drug particle can only pass through the film when the condition mentioned above can be fulfilled.

4.3 Mathematical Model 2:

The condition explained in Mathematical Model 1 depicts an extreme condition, that is when the film is fully stretched and the hollow diamond completely attains a square formation. However, another condition may also be explored, in which a range of particle sizes may pass through the film even before it is fully stretched out to maximum pore size.

If we consider the hollow diamond in one unit cell (see figure 14 a), and apply stretching forces on both ends, as discussed earlier, the geometry of the diamond will be distorted to attain a square form (Figure 8 c). When forces are applied vertically on the diamond ABCD (Figure 14 b), diagonal 'BD' which is equal to Dw , will increase in length, so that the segment 'AC' decreases in length. This will affect the angles at all four vertices of the

polygon so that the four angles move towards 90° , and all the sides of the polygon align in a square configuration. When the hollow space in the film is in the configurations shown in b), BDC will be a right angled triangle. Assuming the base of the triangle to be 'CD', and the perpendicular to be 'BC' and applying the Pythagoras rule, we can conclude that Dw squared will be equal to a sum of the squares of the lengths of segments 'CD' and 'BC'. Since both these segment lengths are sides of a square that are equal in length, we can assign them one variable (x). Therefore,

$$(Dw)^2 = (x)^2 + (x)^2 \quad (2)$$

$$(Dw)^2 = 2x^2 \quad (3)$$

$$Dw = \sqrt{2}.x \quad (4)$$

To account for a range for the general size of drug particles that would be able to pass through the film, the following condition has to be satisfied:

If $Pd=x$, the particle can only pass through when Dw is greater than $\sqrt{2}.x$, that is:

$$Dw > \sqrt{2}.x \quad (5)$$

According to this condition, for any measurement of Dw , the particle size should be less than Pd , that is the following condition should be satisfied:

$$Pd < Dw/\sqrt{2} \quad (6)$$

It may be concluded that the first controlling factor in the release kinetics of drug elution is the pore size of the film, provided that the drug particle sizes satisfy the conditions mentioned above. This may be explored further in a micro scale study of the same model.

Results (Phase II):

Time delay	1st actuation 75ms	2nd actuation 100ms	3rd actuation 125ms	4th actuation 150ms	5th actuation 175ms	6th actuation 200ms	7th actuation 225ms	8th actuation 250ms	9th actuation 275ms	10th actuation 300ms
1	1	4	7	14	14	18	23	21	22	24
2	0	2	4	12	12	18	19	20	23	25
3	0	1	8	15	24	12	14	17	21	24
4	1	4	4	13	13	17	21	21	24	21
5	1	3	1	15	12	16	25	22	21	18
Mean value in grams	0.4	2.8	4.8	13.8	15	16.2	20.4	20.2	22.2	22.4

Table 2. Quantity of drug administered with reference to increasing times for film actuation (Pulley Mechanism)

Time delay	1st actuation 75 ms	2nd actuation 100ms	3rd actuation 125ms	4th actuation 150ms	5th actuation 175ms	6th actuation 200ms	7th actuation 225ms	8th actuation 250ms	9th actuation 275ms	10th actuation 300ms
1	0.5	1	5	1	15	15	23	19	17	31
2	0.6	2	12	6	4	16	17	23	26	28
3	0.8	2	8	8	15	13	11	5	18	15
4	0.9	3	4	7	7	13	11	21	11	23
5	1	1	1	9	20	8	8	13	13	30
Mean Value in grams	0.76	1.8	6	6.2	12.2	13	14	16.2	17	25.4

Table 3. Quantity of drug administered with reference to increasing times for film actuation (Lead Screw Mechanism)

Weight recordings with reference to both mechanisms have been presented in tabular form (above). Since an Arduino microcontroller was used for controlling the milli-second time periods that the motor was powered up for, the entire operation was pre-programmed on an Arduino interface. For each set of five readings, a mean reading was derived, and interpreted graphically as part of a linear trend-line. Mean values corresponding to increasing time intervals of 75 ms to 300 ms for the pulley mechanism range from 0.4 milligrams to 22.4 milligrams. Whereas mean values corresponding to increasing time intervals from 75 ms to 300 ms for the lead screw mechanism range from 0.76 milligrams to 25.4 milligrams. The range therefore, of drug delivered in milligrams is comparable for both mechanisms.

From the results it may be observed that the weights recorded for drug eluted for data sets, show a linearly increasing trend, with increasing time intervals for which the motor is powered up (depicted in figures 15 and 16). A comparison of individual weight recordings can be made with the sequential recordings for each mechanism's data set separately. For example, the time interval is increasing in similar increments of 25 milliseconds; corresponding to that, the increments in each weight recording correspond to a range of 0.2 mg to 4 mg, with two exceptions in each data set where the increment goes up to 9 mg (pulley mechanism) and 8 mg (lead screw mechanism).

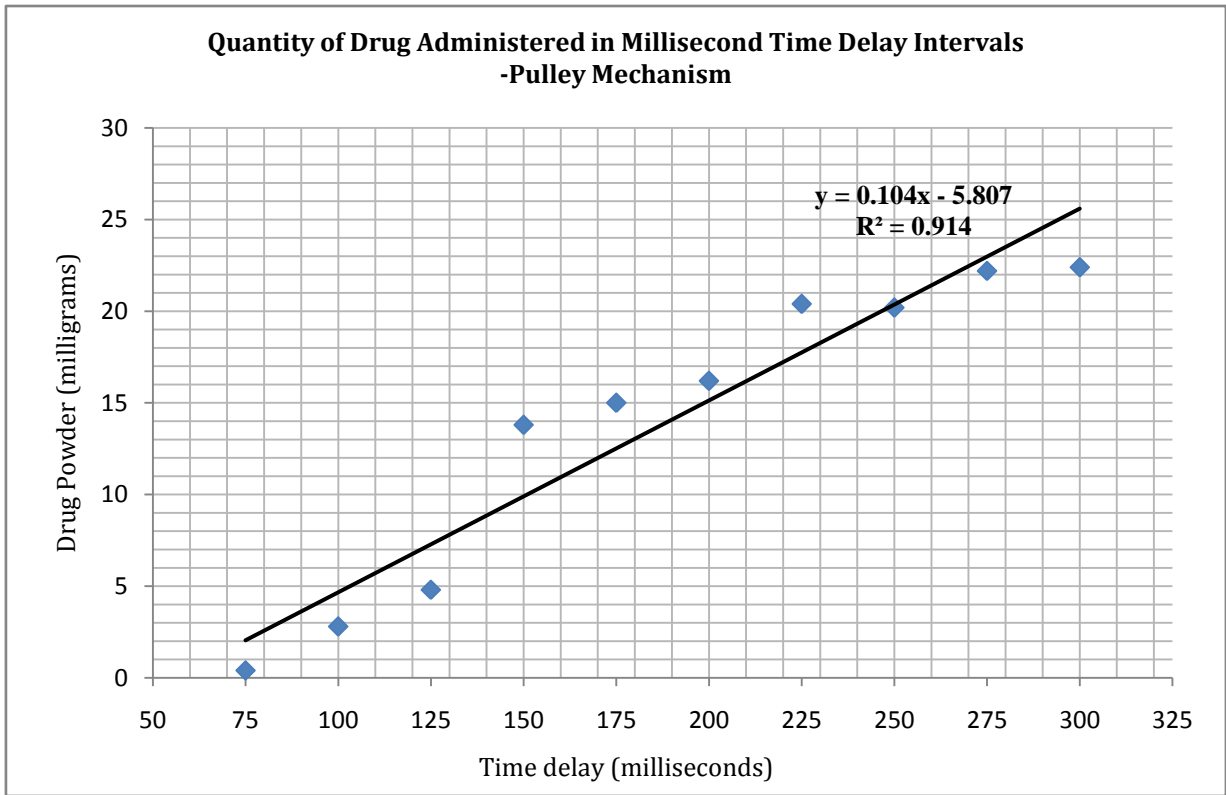


Figure 15: Graphical representation of results; showing the amounts of drug delivered through the string-pulley mechanism

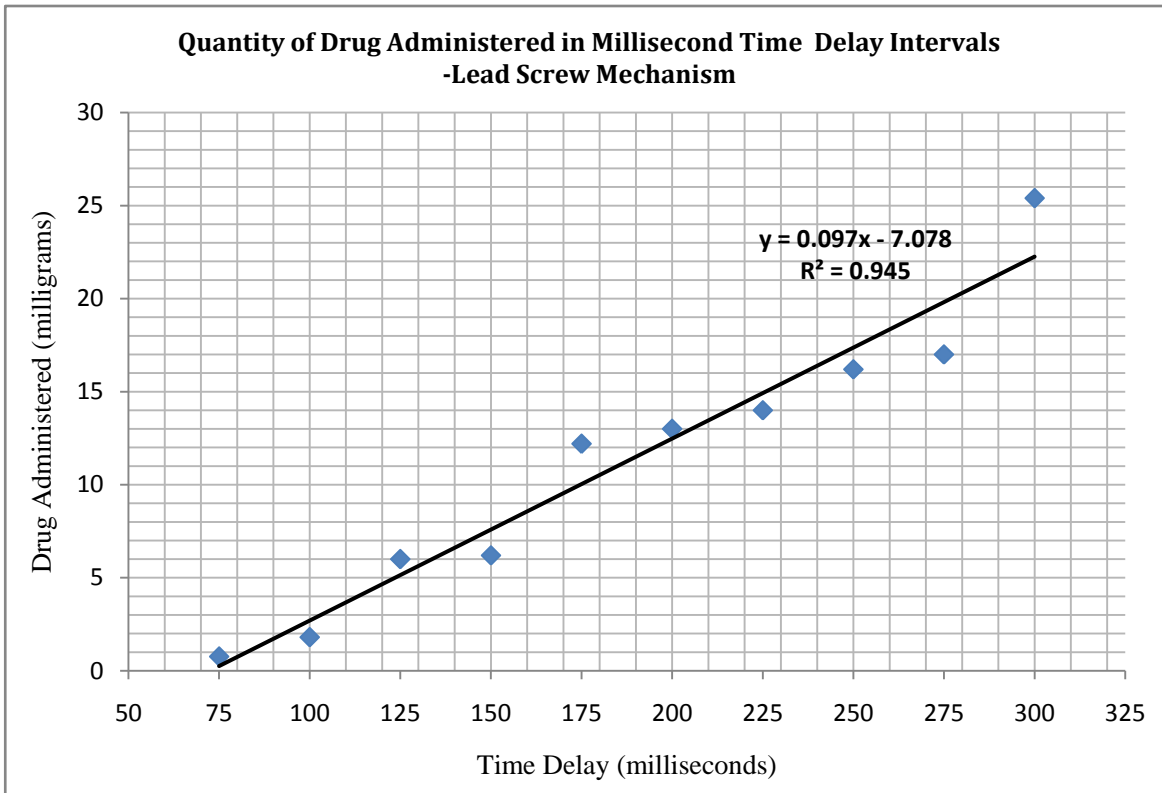


Figure 16: Graphical representation of results; film actuation controlled through the lead-screw mechanism

The scatter pattern for both graphs may be seen in figures 15 and 16. From both graphical representations of drug release patterns it can be deduced that a positive, linear correlation exists between the amount of drug released and the time interval for which the motor is powered up. The slope or flux (that is the pharmaceutical powder released per unit time), is comparable for both mechanisms, that is, 0.104 mg ms^{-1} for the pulley mechanism and 0.097 mg ms^{-1} for the lead screw mechanism. However, a higher regression coefficient (R^2 value) is observed for the lead screw mechanism (0.945) as compared to the pulley mechanism (0.914). A difference of 0.03 between the medicament profiles of both data sets shows that there is a higher linear correlation between the data set related to the lead screw mechanism, and more variance can be accounted for by this regression model.

Mode of Drug Delivery	Rate of Release (mg/ms)	Regression Coefficient for Linear Data (R² value)
Pulley Mechanism	0.104	0.914
Lead-Screw Mechanism	0.097	0.945

Table 4: A comparison of the rate of release (flux or slope of the graph) and regression coefficient values for both data sets

SE added for each reading	SE added (cumulative)	Quantity of SE removal (1)	Quantity of SE removal (2)	Quantity of SE removal (3)	Quantity of SE removal (4)	Quantity of SE removal (average)	Quantity of SE removal (Cumulative)
2ml	2	0.8	1.8	1.2	0.8	1.15	1.15
2ml	4	1.7	1.9	1.8	2	1.85	3
2ml	6	1.8	1.9	1.9	1.9	1.875	4.875
2ml	8	1.8	1.8	1.8	1.85	1.813	6.688
2ml	10	1.8	1.75	1.9	1.95	1.85	8.518

Table 5: Quantity of Simulated Exudate (SE), taken up from the simulated wound site; four data sets were obtained; the values have been averaged

Fluid quantities recorded from the wound exudate tests show that 0.8 ml of the exudate could be drawn up from the device, whereas the initial wound exudate quantity was 2 ml. The amount of exudate that could be drawn up from the device increased in subsequent readings, going up to a maximum of 2 ml, in the last (fourth) set of readings. To simulate real-time wound conditions, fresh SE solution was added to the simulated wound bed after hourly intervals. The absorbent material was allowed to soak up the exudate for 15 minutes, after which the exudate was drawn up from the main absorbent conduit on surface B of the device. A graph between cumulative readings for the amount of exudate present in the

simulated wound bed, against the amount of exudate drawn up from the device has been plotted and shown in figure 17.

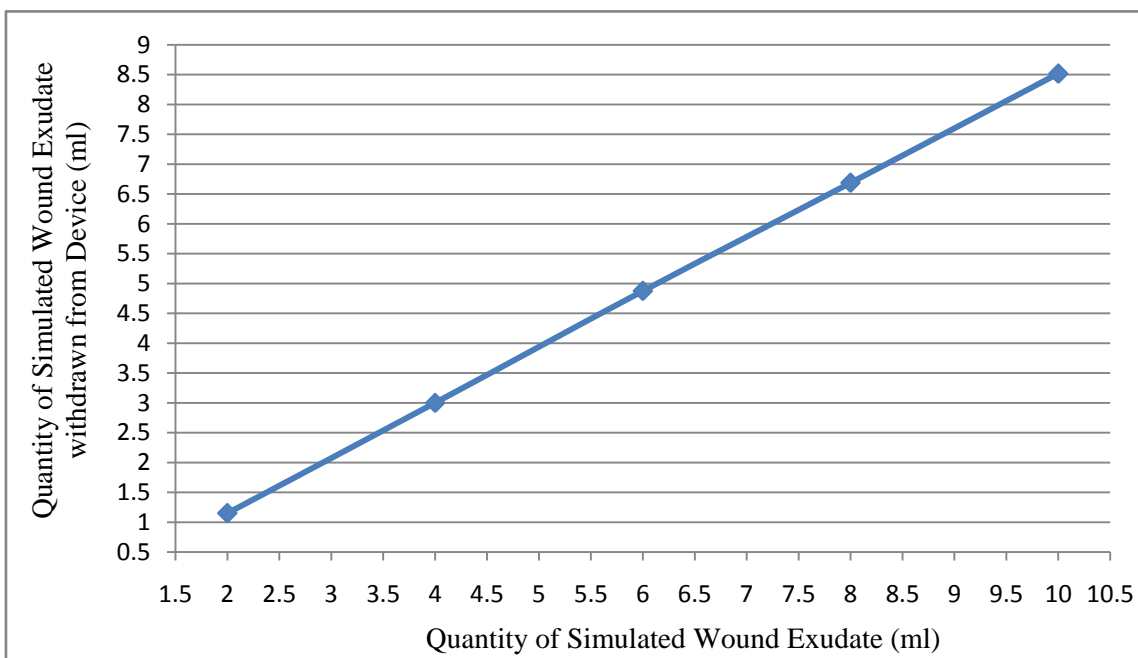


Figure 17: Graphical representation of the quantity of simulated wound exudate drawn up from the device as compared to the quantity of simulated wound exudate present

Phase II of the study reported here aims to investigate the working of a novel wound healing device which hosts multiple functionalities; that is, controlled drug delivery, and exudate removal. The device has been fabricated from flexible, biocompatible polymeric material so that it can complement the contours of the skin surface. An attempt has been made to investigate the possibility of electronically controlling the amount of drug that may reach the site of the medicament, and the results obtained are discussed here. Both mechanisms that are controlling drug delivery, that is, the actuation (extension) of the auxetic film are miniaturized so as to fit compactly into the device, without challenging the size or flexibility of the overall assembly.

In case of both mechanisms a larger time interval means a greater number of revolutions of the motor shaft head, and hence a greater degree of film extension. Since the film that is ultimately controlling (or limiting) the amount of drug that passes through to the site of the wound is auxetic, it means that the exertion of a uni-axial force at one end of the film would

cause the auxetic design to open up in both horizontal (in line of the applied force), and vertical (perpendicular to that of the applied force) directions. This would cause an overall increase in pore size; this would allow medicament (or particulates of any kind) to pass through the film.

When comparing the results of both mechanisms mentioned above, it may be re-iterated that the flux or rate of release for both the pulley and the lead screw mechanism show a positive, linear correlation with the time intervals (for which the motor was powered up). This linearity is an advantage in such a device, since the purpose of electronic actuation for drug delivery is to decrease reliance on abstract mechanisms of drug release such as diffusion or chemical interactions. The linear behavior of the drug release profile means that the release can be predicted, or controlled in precisely timed, pre-programmed intervals. With the exception of a few outliers, (readings at 175 ms), it may be seen that the amounts of powdered medicament that passed through the auxetic film are comparable for both mechanisms. The weight recordings may also be different because in the pulley mechanism, the main factor affecting the actuation of the film is the winding of the string on the motor shaft, however, for the lead screw mechanism, the number of threads per turn on the threaded screw also have a direct affect how far the nut (and hence the beam to which the film is attached) moves, with each rotation of the motor head. Hence pore widening in the auxetic film is directly correlated with this factor as well.

If data sets for both mechanisms are compared, the fact that a larger amount of particulates pass through the film in the instance where the lead screw is actuated for greater time intervals (300 ms) shows that there is an inherent limitation in the pulley mechanism. After the motor head shaft rotates to wind the string, and the string is pulled taut, this tension creates a force that is translated as extension for the auxetic film. However, the tension in the taut string also has the effect of creating an opposing force on the motor shaft, which stops it from rotating further. This effect (which we may call the elastic re-bound effect) has trickled down into several weight recordings in the string-pulley mechanism data set. For instance, in several readings, the opposing tension in the string (caused by the pull of the elastic film) limited the motor shaft from winding the string any further, so that there is only a small difference between the last two readings (22.2 mg for 275 ms interval and 22.4 mg

for 300 ms interval). However, in the lead screw mechanism, no such limitation exists. Hence the last weight recording has gone up to 25.4 mg for 300 ms in this data set.

The flux/rate of release of both the pulley mechanism data set (0.104 mg ms^{-1}), and the lead screw mechanism data set (0.097 mg ms^{-1}) is comparable, with only a nominal difference of 0.007. This is because both mechanisms essentially achieve the same result, that is, an actuation of the film causing an overall extension and widening of the pores that leads to drug particulates passing through.

An analysis of the degree and pattern of scatter points in our graphical interpretation for both data sets reveals that there is a difference in the scatter points for both string-pulley and lead screw data sets. The R^2 value, which depicts the goodness of a fit typically when dealing with linear correlations such as this one, is 0.914 for the pulley mechanism data set, and 0.945 for the lead screw data set. Both values are close to 1, which shows that there is a strong linear correlation between the data. This also shows that a large degree of variance is accounted for by this regression model. These values place our initial observations of predictability of the linear data into perspective. However, the regression coefficient is larger for the lead screw data set (0.945) as compared to the string-pulley data set (0.914). On this basis it may be deduced that the lead screw mechanism is a better suited candidate for such a device, where predictability and control of the dose administered are key considerations.

The main advantage of electronically controlled drug delivery lies in the complete control over when drug should be administered to the patient. Research has been conducted on other preparations [36] where drug release profiles are dependent upon the fabrication technique or chemical linkages with other agents. While offering obvious advantages for wound healing, the fact remains that there is no absolute control over the amount of drug eluting from the formulation/dressing. In the current work, we have used a pharmaceutical diluent to validate the drug release profiles; the amount of the active ingredient administered can thus be varied by varying the composition of the active ingredient in the pharmaceutical powder (drug reservoir). The drug to be administered can be increased, decreased or stopped at will, depending on the requirement of the patient.

The exudate removal efficiency of the device has been tested using an ionic solution (simulated wound exudate) and to simulate real-time wound conditions, 2 ml of the

simulated wound exudate was added to the container to test both the absorbing and exudate removal capacity of the device. It was found that in the first of these series of tests, 0.8 ml of the simulated exudate was drawn up from the device, although 2 ml of the solution was poured into the Petri dish. This could be attributed to the fact that initially, the cellulose absorbent material in the grooves (surface A) of the device was completely dry, and some of the solution remained entrapped in the cellulose fibers. More of the solution was drawn up in later readings; in the fourth set of readings this goes up to 2 ml. This shows that initial exudate draws were less efficient as compared to latter ones. A possible explanation for this could simply be that fluid affinity increases in wet cellulose fibers and because of the cohesive nature of water molecules, more exudate is drawn up in later readings. The absorbent capacity of this device is higher as compared to conventional dressings [40] because of the larger surface area of the grooves, in which the absorbent material is stored. This additional feature of exudate collection from the device also means that the exudate can be examined clinically and drug therapy or dosage regimen can be modified accordingly.

Conclusion:

The macro model for bandage assembly may be studied further on a micro scale and in simulated body conditions in vitro to prove the efficacy of this device for use in tunable drug delivery. For the macro model, as proved by image processing results and the mathematical models given above, this device offers the opportunity of fine tuning control of drug delivery to the wound site, through adjustable porosity of the auxetic film and actuation of the mechanism to which it is attached. Further studies may be conducted to bridle the modulation of release kinetics of the drug to be dispensed through this laminate assembly.

For the miniaturized version, tests have been performed to evaluate both the drug delivery and exudate removal functions for this novel multifunctional wound healing device. A linear relationship has been shown between the amount of drug released and the time for which the electronic drug controlling mechanism is powered. It has been demonstrated that precisely controlled quantities of drug can be administered to the site of injury. In this respect, the lead screw mechanism for controlling drug delivery has shown a stronger linear correlation in the results. Exudate removal tests demonstrate that the device design facilitates efficient removal of simulated wound exudate, and that, like the drug delivery component, this feature can also be tailored according the patient's treatment regime. In future works, an in-vitro biological study may be conducted, and the design of the device may be modified further according to the results, so that this study can be explored further with reference to clinical applications.

References:

1. Majno G. The healing hand: man and wound in the ancient world: Harvard University Press; 1991.
2. Thomas S. Wound management and dressings: Pharmaceutical Pr; 1990.
3. Helfman T, Ovington L, Falanga V. Occlusive dressings and wound healing. Clinics in dermatology 1994;12[1]:121-127.
4. Percival NJ. Classification of wounds and their management. Surgery [Oxford] 2002;20[5]:114-117.
5. Bryant R, Nix D. Acute and chronic wounds: Elsevier Health Sciences; 2006.
6. Mostow EN. Diagnosis and classification of chronic wounds. Clinics in dermatology 1994;12[1]
7. Bolton L, Van Rijswijk L. Wound dressings: meeting clinical and biological needs. Dermatology nursing/Dermatology Nurses' Association 1991;3[3]:146.
8. Krasner D, Kennedy K, Rolstad B, Roma A. The ABCs of wound care dressings. Ostomy/wound management 1993;39[8]:66, 68.
9. Baum CL, Arpey CJ. Normal cutaneous wound healing: clinical correlation with cellular and molecular events. Dermatologic Surgery 2005;31[6]:674-686.
10. Martin P. Wound healing--aiming for perfect skin regeneration. Science 1997;276[5309]:75-81.
11. Gilmore M. Phases of wound healing. Dimensions in oncology nursing: journal of the Division of Nursing 1991;5[3]:32.
12. Vowden K, Vowden P. Understanding exudate management and the role of exudate in the healing process. British Journal of Community Nursing 2003;8[11 [Exudate Suppl 2]]:4-13.
13. Krasner D. Minimizing factors that impair wound healing: a nursing approach. Ostomy/wound management 1995;41[1]:22.
14. Winter GD. Formation of the scab and the rate of epithelization of superficial wounds in the skin of the young domestic pig. 1962.
15. Dyson M, Young S, Pendle CL, Webster DF, Lang SM. Comparison of the effects of moist and dry conditions on dermal repair. Journal of investigative dermatology 1988;91[5]:434-439.
16. Rovee DT, Kurowsky CA, Labun J. Local wound environment and epidermal healing: Mitotic response. Archives of Dermatology 1972;106[3]:330.
17. Atiyeh BS, El-MUSA KA, Dham R. Scar Quality and Physiologic Barrier Function Restoration After Moist and Moist-Exposed Dressings of Partial-Thickness Wounds. Dermatologic Surgery 2003;29[1]:14-20.

18. Atiyeh BS, Amm CA, El Musa KA. Improved scar quality following primary and secondary healing of cutaneous wounds. *Aesthetic plastic surgery* 2003;27[5]:411-417.
19. Flanagan M, Marks-Maran DJ. *Wound management*: Churchill Livingstone; 1997.
20. Rheinecker SB. Wound management: the occlusive dressing. *Journal of athletic training* 1995;30[2]:143.
21. Mertz P, Davis S, Cazzaniga A, Cheng K, Reich J, Eaglstein W. ELECTRICAL-STIMULATION-ACCELERATION OF SOFT-TISSUE REPAIR BY VARYING THE POLARITY. *WOUNDS-A COMPENDIUM OF CLINICAL RESEARCH AND PRACTICE* 1993;5[3]:153-159.
22. Falanga V, Bourguignon G, Bourguignon L. Electrical stimulation increases the expression of fibroblast receptors for transforming growth factor-beta. *J Invest Dermatol* 1987;88[4]:4-6.
23. Khil MS, Cha DI, Kim HY, Kim IS, Bhattarai N. Electrospun nanofibrous polyurethane membrane as wound dressing. *Journal of Biomedical Materials Research Part B: Applied Biomaterials* 2003;67[2]:675-679
24. S. Guo, L.A. DiPietro, Factors affecting wound healing., *J. Dent. Res.* 89 (2010) 219–29.
25. C.T. Hess, Practice Points Checklist for Factors Affecting Wound Healing, 24 (2008) 17112.
26. T.J. Koh, L.A. DiPietro, Inflammation and wound healing: the role of the macrophage., *Expert Rev. Mol. Med.* 13 (2011) e23.
27. A. Sindrilaru, T. Peters, S. Wieschalka, C. Baican, A. Baican, H. Peter, et al., An unrestrained proinflammatory M1 macrophage population induced by iron impairs wound healing in humans and mice, 121 (2011) 985–997.
28. B. a Lipsky, C. Hoey, Topical antimicrobial therapy for treating chronic wounds., *Clin. Infect. Dis.* 49 (2009) 1541–9.
29. R. Sripriya, M.S. Kumar, M.R. Ahmed, P.K. Sehgal, Collagen bilayer dressing with ciprofloxacin, an effective system for infected wound healing., *J. Biomater. Sci. Polym. Ed.* 18 (2007) 335–51.
30. Polymers in Controlled Drug Delivery | MDDI Medical Device and Diagnostic Industry News Products and Suppliers
31. R. LANGER, INVITED REVIEW POLYMERIC DELIVERY SYSTEMS FOR CONTROLLED DRUG RELEASE, *Chem. Eng. Commun.* 6 (1980) 1–48.

32. H. Search, C. Journals, A. Contact, M. Iopscience, I.P. Address, Microporous materials with negative Poisson ' s ratios . I . Microstructure and mechanical properties, 1877 (1877).
33. A. Alderson, UBIR : University of Bolton Institutional Repository Modelling of the mechanical and mass transport properties of auxetic molecular sieves : an idealised organic (polymeric honeycomb) host-guest system ., (2005).
34. Expanding Materials and Applications: Exploiting Auxetic Textiles - Science News - redOrbit,
35. C.D. Tran, Cellulose, Chitosan and Keratin Composite Materials. Controlled Release of Drug., Langmuir. (2014).
36. R. a Thakur, C. a Florek, J. Kohn, B.B. Michniak, Electrospun nanofibrous polymeric scaffold with targeted drug release profiles for potential application as wound dressing., Int. J. Pharm. 364 (2008) 87–93.
37. A. Alderson, J. Rasburn, S. Ameer-Beg, P.G. Mullarkey, W. Perrie, K.E. Evans, An Auxetic Filter: A Tuneable Filter Displaying Enhanced Size Selectivity or Defouling Properties, Ind. Eng. Chem. Res. 39 (2000) 654–665.
38. a. Alderson, J. Rasburn, K.E. Evans, Mass transport properties of auxetic (negative Poisson's ratio) foams, Phys. Status Solidi. 244 (2007)
39. D. Attard, E. Manicaro, R. Gatt, J.N. Grima, On the properties of auxetic rotating stretching squares, Phys. Status Solidi. 246 (2009)
40. An “in-vitro” comparison of the physical characteristics of hydrocolloids, hydrogels, foams, and alginate / cmc fibrous Product groups tested, 1–24.